GaN growth on (111) Si with very thin amorphous SiN layer by ECR plasma-assisted MBE

Masao Tamura, Máximo López-López
Physics Department, Centro de Investigación y de Estudios Avanzados del IPN, Apartado Postal 14-740, 07000 Mexico, D. F., Mexico

Tokuo Yodo
Electronic Engineering, Osaka Institute of Technology 5-16-1 Omiya, Asahi-ku, Osaka 535-8585, Japan

We have investigated the structure and quality of GaN films grown on a 2-3 nm thick amorphous SiN layer formed on (111) Si by electron cyclotron resonance plasma-assisted molecular beam epitaxy under various growth conditions by using both conventional and high-resolution transmission electron microscopy. It is shown that (0001) hexagonal GaN (α-GaN) films are epitaxially grown on the above-mentioned substrates under optimum growth conditions. With the deviation of optimum conditions, GaN films present rough surface and are composed of small grains of an average size of 0.1 µm. Further, for the growth of decreased effective ratio of nitrogen radical molecules in nitrogen gas, the growth of cubic GaN is predominantly detected with α-GaN. High density pure-edge threading dislocations observed in α-GaN films are considered to be generated due to island-island coalescence at an early stage of growth.

Keywords: GaN; Si; Molecular beam epitaxy; Transmission electron microscopy

1. Introduction

The good quality heteroepitaxial films of GaN on Si are very attractive, if we consider the application for the combination of optoelectronic properties of GaN with highly advanced Si electronic devices. Furthermore, compared to popular substrates for GaN growth such as sapphire or SiC, Si substrates have several advantages; they provide low-cost and large size wafers, good electrical conduction, high crystalline perfection, etc. In general, GaN crystallizes in either the stable hexagonal (α-GaN) or the metastable cubic (β-GaN) phase, depending on (111) or (001) Si substrates. The crucial problem of the direct growth of GaN on Si is the formation of amorphous silicon nitride (SiN) at the GaN/Si interface [1, 2] together with the large lattice mismatch (~17 %) and the large difference in thermal expansion coefficients (~3 x 10^{-6}/k). The residual nitrogen gas in the growth chamber or active nitrogen flux for using the growth of GaN easily react with Si, resulting in the SiN formation on Si substrate surfaces [2]. To overcome this problem, the growth of various kinds of intermediate buffer layers such as SiC, AlN, GaAs, AlAs and Al_2O_3 has been successfully applied for the growth of high quality GaN on Si [1].

Nakada et al. [3] have shown that α-GaN was epitaxially grown on (111) Si without the use of the above-mentioned buffer layers by RF plasma-assisted molecular beam epitaxy (MBE). In this case, a 1-1.5 nm thick SiN layer remained at the GaN/Si interface. However, detailed structural properties of the GaN layers thus grown have not been clarified.

In the present study, we carried out conventional cross-sectional transmission electron microscope (XTEM) and plan-view TEM (PTEM) observations, and high-resolution XTEM (HRXTEM) observations for electron cyclotron resonance (ECR) plasma-assisted MBE grown GaN films on (111) Si substrates under various growth conditions. The main purpose of this paper is to report the characteristics of lattice defects in α-GaN grown on (111) Si having a thin amorphous SiN layer as well as to discuss their generation. We also report the effect of the thickness of SiN layer and other growth parameters on the quality of grown films.

2. Experimental procedures

GaN layers were grown in a conventional MBE system equipped with an ECR-activated nitrogen plasma source. The substrates used were lightly n-doped (111) Si wafers. After the native oxides on substrate surfaces were etched in a buffered HF solution, they were loaded into an MBE chamber and were thermally cleaned at 1250 °C for 5 min. Then, GaN films were grown under various growth conditions such as ECR plasma power, nitrogen gas flow rate, Ga-cell temperature, substrate temperature and nitridation time at 800 °C. These growth parameters were changed except for a fixed plasma power of 350 W as listed in Table 1.

Table 1. Parameters used in the samples growth

ECR plasma power	350 W
Nitrogen gas flow rate	1.5 – 8 sccm
Ga cell temperature	1000 – 1055 °C
Substrate temperature	650 – 900 °C
Nitridation time	0 – 60 min.

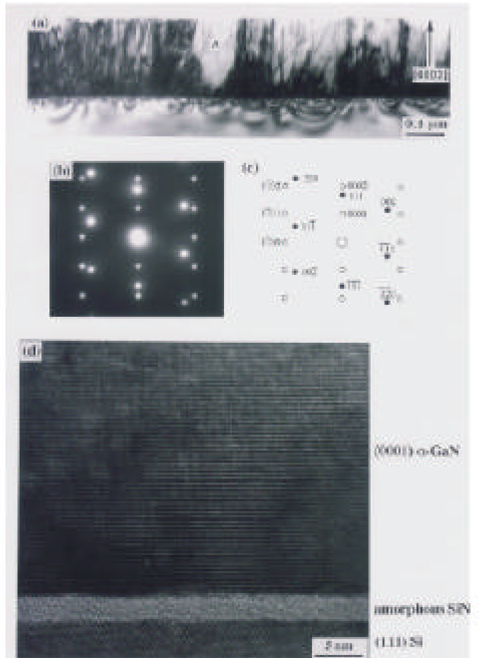

Figure 1 (a) Bright field XTEM micrograph of 0.2 ìm thick α-GaN on (111) Si. The GaN and Si are viewed in the $[11\bar{2}0]$ and $[1\bar{1}0]$ projections, respectively. Two-beam conditions with **g** = [0002]. Region A is slightly misoriented against the surrounding area. (b) TED pattern from the interface region of (a). (c) Corresponding sketch of (b) and basic reflection spots are indexed for GaN (o) and Si (•). ○ is a direct spot. The {0001} GaN and {002} Si reflections are observable due to double diffraction. (d) HRXTEM micrograph of the interface region of (a). Almost defect free α-GaN layer is seen to be epitaxially grown on 2.5 nm thick amorphized (111) Si.

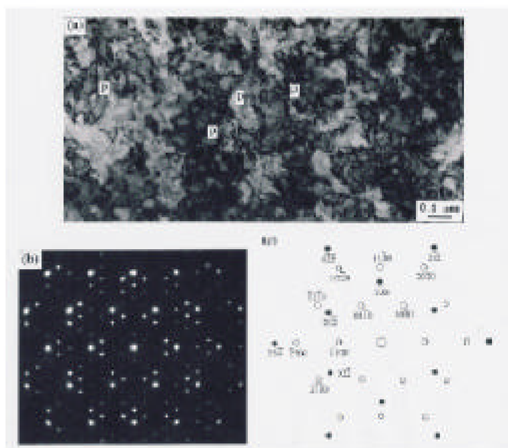

Figure 2 (a) Bright field PTEM micrograph of a Fig.1 sample. Multi-beam imaging conditions were used to avoid defect invisibility. Some planar defects are denoted by P. (b) TED pattern from both (0001) α-GaN and (111) Si of (a). (c) Corresponding sketch of basic reflection spots of (b), and are indexed for GaN (o) and Si (•). ○ is a direct spot. Extra spots seen in (b) except for basic reflection spots are due to double diffraction.

In an optical emission spectrum for ECR nitrogen plasma at a plasma power of 350 W, we mainly paid our attention to two emission lines at 357 and 391 nm. The former emission at 357 nm is due to nitrogen radical molecules ($N2^*$) in the 2nd positive series of an emission spectrum [4] and its intensity strongly affected the growth rate of GaN [5]. In a usual GaN growth, we kept the intensity of this emission at a constant value of 320 arb.units. On the other hand, the latter emission at 391 nm is from nitrogen molecular ions ($N2^+$). Therefore, the intensity of this emission strongly influenced the quality of growing layers [6, 7]. We kept this intensity at a low value of 100 arb. units during growth to avoid the introduction of damage into films by $N2^+$ bombardment as much as possible. Nevertheless, we sometimes observed the formation of extended defects in GaN layers probably due to a small fluctuation of the emission during growth as will be described in section 6.1.

The structure and quality of GaN layers were studied at 200 keV by conventional XTEM and PTEM observations, and HRXTEM observations. The cross-sectional specimens were prepared by mechanical gliding, followed by 4 keV Ar ion beam bombardment with a beam current of 1 mA (total) and an incident angle of 12°.

3. General features of GaN films grown under optimum growth conditions

We describe here typical characteristics of GaN films grown under optimum conditions of representative growth parameters; i.e. ECR plasma power, nitrogen gas flow rate, Ga cell temperature, substrate temperature and nitridation time. They were set at 350 W, 2 sccm, 1041 °C, 800 °C and 5 min, respectively.

Figures 1 (a) and (b) show bright-field XTEM micrograph of 0.2 µm thick (0001) α–GaN layer grown on (111) Si and corresponding transmission electron diffraction (TED) pattern obtained from the interface region between GaN and Si, respectively. Also, in Fig. 1(c), typical indices of diffraction spots from both GaN and Si of Fig. 1(b) are indicated. Figure 1(d) also shows HRXTEM micrograph of the interface region of Fig. 1(a), clearly indicating the formation of a continuous and atomically flat 2.5 nm thick amorphous SiN layer on Si surface.

From all of the results of Fig. 1, we can say as follows: (1) Even if there exists a 2.5 nm thick amorphous SiN layer on (111) Si substrate (the layer thickness in this case is twice as thick as the result of Nakada et al. [3]), (0001) α–GaN was epitaxially grown on (111) Si with an epitaxial relationship of $[11\bar{2}0]$*GaN* // $[1\bar{1}0]$*Si*, as has also been observed by Nakada et al.[3]. (2) Threading defects with a high density were observed (Fig.1 (a)), the same as those in α–GaN grown on (111) Si having an AlN buffer layer by MOCVD [8, 9] and MBE [10], but no appreciable streaking of diffraction spots along the [0001] direction from α–GaN

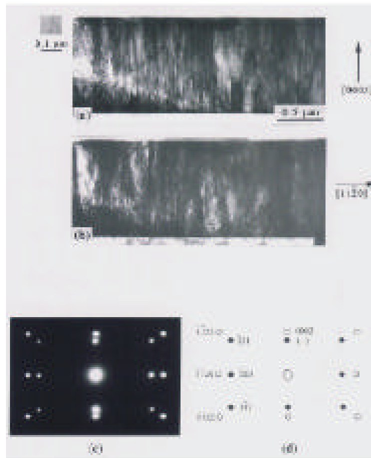

Figure 3 (a) and (b) are bright field XTEM micrographs of 1.1 μm thick α-GaN on (111) Si. The GaN and Si are viewed in the [1 $\bar{1}$ 00] and [11 $\bar{2}$] projections, respectively. (a) **g** = [0002] and (b) **g** = [11 $\bar{2}$ 0] reflections from GaN. The enlarged micrograph of dislocation loops is inserted in (a). (c) TED pattern from the interface region between GaN and Si. (d) Corresponding sketch of (c) and basic reflection spots are indexed for GaN (o) and Si (•). ○ is a direct spot.

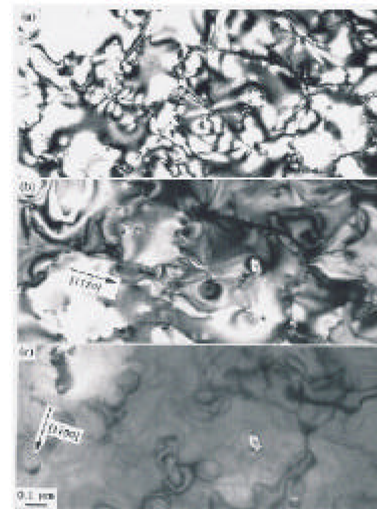

Figure 4 Bright field PTEM micrographs of a Fig. 3 sample which were taken for the same region. (a) multi-beam conditions and two-beam conditions with (b) **g** = [11 $\bar{2}$ 0] and (c) **g** = [1 $\bar{1}$ 00].

(Fig.1(b)) indicates that the (0001) basal plane faults (stacking disorders) are low density, contrary to the results of GaN on Si with an AlN buffer by MBE [10].

Figure 2 (a) shows PTEM micrograph of the same sample of Fig.1 and Fig. 2 (b) is corresponding TED pattern from both (111) Si and (0001) α–GaN. Figure 2 (c) is its schematic sketch of basic reflection spots from Si and GaN except for double diffraction spots. The PTEM micrograph shows the high-density of threading dislocations and some planar defects that penetrate to the top surface of the sample. In particular, we note the formation of low angle grain boundaries that are formed by dislocations (the nature of dislocations is described in connection with Figs. 3 and 4). The grain sizes vary from about 0.1 to about 0.3 μm. The twist around the c-axis of these grains is very small, as suggested from diffraction spots in Fig. 2(b). It was estimated that in-plane misorientation of the grains is less than 3°. The TED pattern clearly shows in-plane orientation relationship of [11 $\bar{2}$ 0]*GaN* // [1 $\bar{1}$ 0]*Si* and [1 $\bar{1}$ 00]*GaN* // [11 $\bar{2}$]*Si* between (0001) α-GaN and (111) Si, as already shown in a cross-section sample of Fig. 1(b).

Figures 3 (a) and (b) show XTEM micrographs of a 1.1 μm thick grown α-GaN layer on (111) Si under the same growth conditions for a Fig. 1 sample. In this case, the TEM specimen was prepared from the [1 $\bar{1}$ 00] GaN and [11 $\bar{2}$] Si orientations, as shown in TED pattern of Fig. 3(c), which was obtained from the interface region between GaN and Si. Figure 3(d) also indicates typical indices of diffraction spots from both GaN and Si of Fig. 3(c). The dark line (Figs. 3(a) and (b)) seen at the location of about 0.1 μm below the surface consists of dislocation loops. In Fig. 3 (a), a part of elongated micrograph of the loops is inserted. We describe the reason for the formation of these extended defects in section 6.1.

Both XTEM micrographs of Fig. 3 were taken under two-beam bright-field conditions of (a) **g** = [0002] of α-GaN and (b) **g** = [11 $\bar{2}$ 0] of α-GaN for the same region. This set of two XTEM micrographs allows us to suppose the nature of dislocations on the basis of the **g**·**b** = 0 criterion, although a very high density of dislocations running along the [0001] direction exists. On the other hand, it is already established [11] that there exist three types of threading dislocations (TDs) in α-GaN: TDs having pure-edge character (Burgers vector **b** = 1/3 <11 $\bar{2}$ 0>), TDs having pure-screw character (**b** = <0001>) and TDs having mixed character (**b** = 1/3 <11 $\bar{2}$ 3>). The density of the dislocations in Fig. 3(a) is lower than that in Fig. 3(b). This indicates that the dislocations having pure edge character are more than those having pure screw and mixed characters, although the latter two types of dislocations are still observed in high density.

The pure-edge dislocations can most effectively relax in-plane misorientations between small angle grain boundaries. This was also confirmed for the bright-field PTEM micrographs as shown in Fig.4, the PTEM sample of which was prepared from the same sample of Fig. 3. The PTEM micrographs of Fig. 4 again show the formation of subgrains. Almost all the dislocation images forming subgrains are out of contrast in Fig. 4(c) and are visible in Fig. 4(b). This suggests that dislocations forming grain boundaries are pure-edge or mixed dislocations. Taking into consideration the XTEM results of Fig. 3, it can be inferred that pure-edge dislocations mainly compose grain boundaries. Also, if we compare Fig. 4(a) with Fig. 2(a), it can be understood that the subgrain size increases with

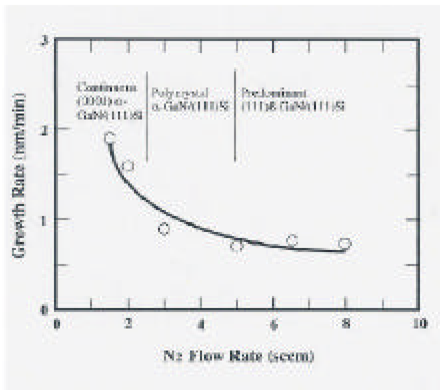

Figure 5 Growth rate of GaN as a function of N_2 gas flow rate.

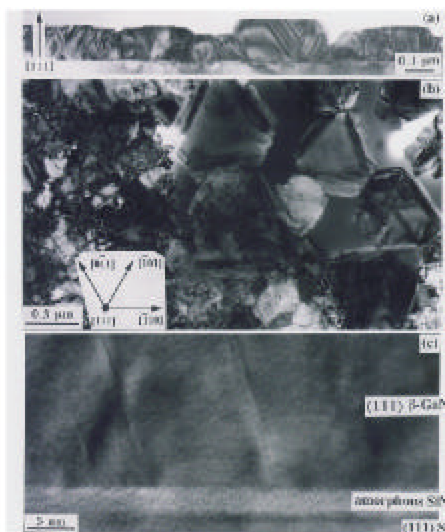

Figure 6 (a) Bright field XTEM micrograph of (111) β-GaN on (111) Si observed from the [11 $\bar{2}$] direction. Two-beam conditions with **g** = [111]. (b) Bright field PTEM micrograph of a sample (a). Multi-beam conditions. (c) HRXTEM micrograph of the interface region between (111) β-GaN and (111) Si observed from the [1 $\bar{1}$ 0] direction.

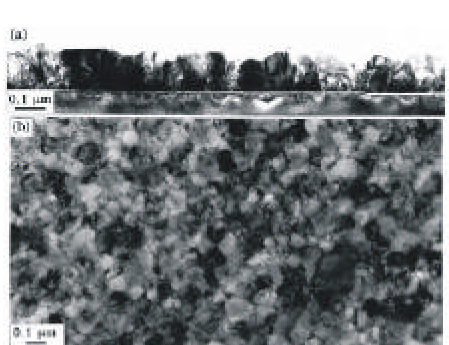

Figure 7 Bright field (a) XTEM and (b) PTEM micrographs of polycrystals of α-GaN on (111) Si. (a) was observed from the [1 $\bar{1}$ 0] direction of Si. (b) Multi-beam conditions.

the increase of film thickness. Rough estimation of grain sizes showed that they are three times larger in Fig. 4 (a) than in Fig. 2 (a).

4. Effect of growth parameters on the structure and quality of grown layers

Figure 5 shows the growth rate of GaN as a function of N_2 gas flow rate. In this experiment, the substrate temperature and Ga-cell temperature were kept constant at 800 and 1041 °C, respectively. We also kept constant the emission intensity at 357 nm due to N_2^* at 320 arb. units. The growth rate clearly decreased with the increase of N_2 flow rate, which suggests that the effective N_2^* ratio included in inert nitrogen gas strongly governs the growth rate of GaN [5].

Under these growth conditions, as the effective ratio of N_2^* in N_2 gas decreases, the growth of β-GaN was remarkably detected together with α-GaN. In particular, for the growth with a density of N_2^* smaller than ~60 arb. units/sccm (for N_2 flow rate higher than 5 sccm in Fig. 5), β-GaN growth on (111) Si was predominantly observed by TEM. In other words, the change of growth conditions from N-rich to Ga-rich induced the β-GaN formation [12].

Figure 6 (a) shows one example of XTEM micrographs of (111) β-GaN on (111) Si obtained for an N_2 flow rate of 6.5 sccm (50 arb. units/sccm of N_2^*) in Fig. 5, which was observed from the [11 $\bar{2}$] direction. Compared to the results of α-GaN of Figs. 1 and 3, it is clear that the main lattice defects generated in β-GaN are planar defects such as stacking faults and twins, instead of threading dislocations in α-GaN. They mainly exist on inclined {111} planes, and faceted {111} planes are also seen at the sides of coalesced islands. Figure 6 (b) is a PTEM micrograph of a Fig. 6 (a) sample. We can see the formation of big isolated islands having a size of about 0.5 μm in the micrograph, the sides of which consist of intersections of faceted {111} planes with the (111) surface of Si. Not only in each isolated island but also in the region of a continuous layer, the generation of planar defects along the <110> directions is seen. It can also be recognized that the individual islands before coalescence are slightly rotated within 10° around the <111> growth axis. Figure 6 (c) shows HRXTEM micrograph near the interface region between β-GaN and Si, observed from the [1 $\bar{1}$ 0] direction. It is understood that (1) (111) β-GaN is epitaxially grown on 2.5 nm thick amorphized (111) Si and (2) planar defects are generated on the inclined {111} plane from the interface.

On the other hand, in the region of an N_2 flow rate between 3 and 5 sccm in Fig. 5, α-GaN was predominantly grown on (111) Si but the grown layer showed uneven surface and consisted of randomly oriented grains. Figures 7 (a) and (b) show one example of XTEM and PTEM micrographs obtained for the sample grown at an N_2 flow rate of 4 sccm. The results indicate that the layer has rough surface having an irregularity of several

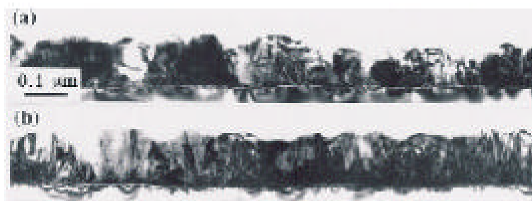

Figure 8. Bright field XTEM micrographs of α-GaN grown on (111) Si substrates which were treated by nitridation time for (a) 0 and (b) 60 min.

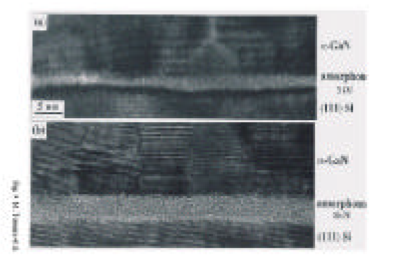

Figure 9. HRXTEM micrographs of the interface regions of Figs. 8 (a) and (b), which correspond to (a) and (b), respectively, observed from the [1 $\bar{1}$ 0] direction of Si.

tens nm and composes of small grains of an average size of 0.1 μm. In Fig. 5, the characteristic region of the structure and quality of GaN thus observed as a function of N_2 flow rate is also shown.

Such a change of crystal quality from continuous single crystal to polycrystal grain growth of α-GaN was also observed for a change of Ga-cell temperature in the range between 1010 and 1055 °C under an N_2 flow rate of 2 sccm and a substrate temperature of 800 °C. With lower temperatures than 1030 °C, grain growth as shown in Fig. 7 was observed, while a single crystal film of (0001) α-GaN was obtained for Ga-cell temperature higher than 1040°C. Predominant β-GaN growth was not detected for the growth of the Ga-cell temperature range used in the experiment. Also, the substrate temperature employed in the range between 650 and 900°C influenced the crystal quality of α-GaN on (111) Si. Generally, at the substrate temperature lower than 750 °C, the formation of Ga-droplets and polycrystal grains was remarkably observed. Therefore, the optimum N_2 flow rate, and Ga-cell and substrate temperatures in the present experiments, in which the continuous single crystal of (0001) α-GaN as described in section 2 was obtained, were 2 sccm (under an intensity of 320 arb. units at a 357 nm emission due to $N2^*$), 1041 and 800 °C, respectively.

5. Effect of nitridation time on the structure and quality of grown layers

In order to study the effect of the SiN layer formation on Si substrates on the quality of grown GaN layers, we prepared the different substrates for which we varied their surface conditions by changing the nitridation time at the duration of 0, 2, 5, 15, 30 and 60 min at 800 °C. Immediately after the nitridation, the growth of GaN was subsequently followed under the same growth conditions as those in section 2. Nitridation was conducted by the same active nitrogen plasma used for the GaN growth.

Figures 8 (a) and (b) show conventional XTEM micrographs taken for α-GaN grown on (111) Si substrates which were treated by nitridation time for 0 and 60 min, respectively. Figures 9 (a) and (b) show HRXTEM micrographs of the interface regions of corresponding samples of Figs. 8 (a) and (b). In this case, nitridation time 0 means that GaN growth was started by the simultaneous supply of Ga and N just after thermal cleaning of substrates in the MBE chamber. We clearly note from Fig. 9 (a) that a non-uniform 2nm thick amorphous SiN layer is formed at the interface. This result suggests that Si surface easily react with nitrogen plasma at the initial stage of GaN growth, resulting in the SiN layer formation. In fact, some authors have previously shown the formation of amorphous SiN on Si substrates at different temperatures of 600 °C [13] and 1000 °C [9], and by different nitrogen species of RF-activated nitrogen [13] and ammonia (NH3) [9] with no special intentional nitridation procedures.

The film grown on the substrate without an intentional nitridation procedure was polycrystalline, which consist of α-GaN grains of about 0.1 μm size as seen in Fig. 8 (a), although <0001> oriented-single crystal α-GaN was grown in a limited region (Fig.9 (a)). On the other hand, in the case that intentional nitridation was done for substrates at times for longer than 15 min, a flat and continuous amorphous SiN layer was formed at the Si surface. In Fig. 9 (b), one example of this case is shown for the result of nitridation time for 60 min. The micrograph reveals the formation of an approximate 3.5 nm thick amorphous SiN layer with very sharp interfaces for an upper and lower material. The increase of the layer thickness with the increase of nitridation time from 15 to 60 min was hardly detected in the HRXTEM micrographs. Compared to the growth on the substrates without an intentional nitridation procedure, the surface roughness of the grown film was improved and the average size of individual grains was increased two or three times (Fig. 8 (b)). The <0001>-oriented α-GaN growth was still observed (Fig. 9 (b)) but discontinuity of the film divided by boundaries was also seen near the interface region. In the present experiment, the optimum nitridation time which led to the flat and continuous α-GaN growth was between 2 and 5 min. As already shown in Figs. 1 (a) and (d), for example, <0001>-oriented single crystal film with a flat surface was epitaxially grown on (111) Si having a 2.5 nm thick amorphous SiN layer.

The interesting issue is that, in spite of no direct bonding between Si and GaN, epitaxial growth of (0001) α-GaN

occurred on (111) Si, maintaining the epitaxial relationship as described before. In other heteroepitaxial systems such as GaAs on Si [14] and GaN on sapphire [15], for example, two step growth procedures, in which thin amorphous-like buffer layers are first grown at a relatively low-temperature and subsequently high-temperature epitaxial growth is carried out, have been widely used and good quality of epitaxial films has been obtained. In these cases, however, thin amorphous-like films which are first deposited, could be recovered into single crystals through a mechanism of solid-phase epitaxy during the second step growth. Therefore, no amorphous layers remain at the interface between film and substrate after the completion of high-temperature epitaxial growth.

Similarly, Ishida et al. [16] reported that for the growth of (001) Si on ($01\bar{1}2$) sapphire by the CVD method, pre-deposition of 1-5 nm thick amorphous Si (sputter-deposition at room temperature) was very effective for obtaining high quality of epitaxial films compared to the direct growth of Si on sapphire. They claimed that the thickness of amorphous Si is crucial to get a good result, although amorphous Si was not recovered into single crystals only by high-temperature heat treatment. However, after the final growth of Si by CVD, they confirmed the formation of single crystal Si near the interface region by the combination of controlled chemical etching with RHEED observations. So, the detailed mechanism of single crystallization of amorphous Si was not clear but the ordered bonding between Si and sapphire was finally realized.

Compared to the results mentioned above, the present case that an intermediate amorphous layer exists between ordered single crystals of GaN and Si, cannot be explained by the previous results. It seems likely that a strong effect of substrate orientation on the achievement of preferred orientation of grown films might work through a thin amorphous layer for the present system. Figure 10 shows an initial growth stage of α-GaN deposited for 3 min (average thickness is about 5 nm) under the same conditions as those in section 2. Triangle islands of α-GaN are grown, showing the formation of one part of (0001) hexagonal shape. One edge of the triangles is directed to the $<11\bar{2}0>$ which is parallel to the <110> direction of (111) Si. Thus, at the beginning stage of the growth, epitaxial relationship of α-GaN is already established by the effect of the underlying (111) Si through an amorphous layer. By considering the results of Figs. 10 and 12, we propose a "pinhole model" for the growth of GaN on Si with a SiN amorphous layer. This model is described in the Appendix. In the present experiment, we could not detect any region of a crystallized SiN layer at the interface, contrast to the result by Nakada et al. [3]. So, there is no possibility that GaN was crystallized through crystalline SiN and underlying (111) Si. Further study is much needed to clarify the detailed mechanism of epitaxial growth on single crystal substrate having a thin amorphous layer together with the effect of an optimum thickness of an amorphous layer on obtaining epitaxial films.

6. Defects introduction

6.1 Extended defects (Dislocation loops)

As stated in experimental procedures, ECR-nitrogen plasma includes energetic molecular ions of N_2^+ at 391 nm in an emission spectrum. These ions are considered to have kinetic energies of 25 - 40 eV [6]. Therefore, these ionic species in the nitrogen plasma have a profound effect on the growth mode, surface morphology, photoluminescence properties and the full-width at half maximum (FWHM) of X-ray diffraction spectra [6, 7]. In other words, low-energy ion bombardment of N_2^+ deteriorates the crystal quality of GaN during growth. We controlled the emission intensity of N_2^+ as low as possible during growth. However, the formation of extended defects (dislocation loops) was sometimes observed in the grown layers, which were considered to be induced by the effect of these energetic ions.

Figure 11 (a) shows one example of HRXTEM micrographs of dislocation loops inserted in Fig. 3 (a). We can clearly see some areas of distorted lattices on (0001) basal planes, the sizes of which are approximately 5 nm in width. In the region surrounded by a square in the figure, we can also notice the dotted white contrast along the [0001] direction. Figure 11 (b) is an enlarged micrograph of this area. In the region near the dotted contrast, the (0001) basal planes are also distorted. In particular, an extra half plane is inserted, as indicated by an arrow. This extra plane extends about 20 nm in length on (0001) plane. These extra half planes are observed in other areas in the figure. They are thought to be produced by the precipitation of interstitial atoms caused by the bombardment of energetic ions. In order to avoid the introduction of such extended defects, we have to pay a careful attention to the stability of nitrogen plasma emission during growth.

6.2 Threading dislocations

In the present GaN growth on Si having a thin amorphous layer, there is no direct bonding between two materials. So, interfacial misfit dislocations due to a large lattice mismatch (~17%) between GaN and Si will not be generated. For example, lattice distortion of GaN and Si is not observed at the interface in the HRXTEM micrograph of Fig. 1 (d). From this fact, it is said that threading dislocations are not dislocations which were formed as a result of bending of misfit dislocations onto $\{10\bar{1}0\}$ prismatic planes and moving toward the [0001] direction.

Figure 12 shows a bright-field PTEM micrograph of α-GaN on (111) Si deposited for 30 min. This stage is one example of coalescening stages among large islands. In

Figure 10. Bright field PTEM micrograph showing the characteristic triangle islands of α-GaN on (111) Si. Growth time was 3 min. Multi-beam conditions.

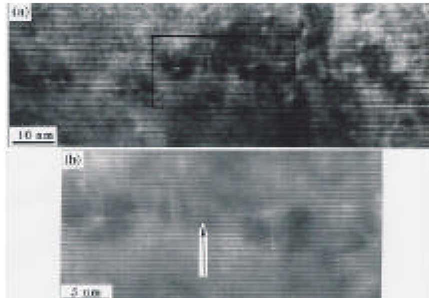

Figure 11. HRXTEM micrographs of dislocation loops inserted in Fig. 3 (a). (b) is an enlarged micrograph of a squared area in (a).

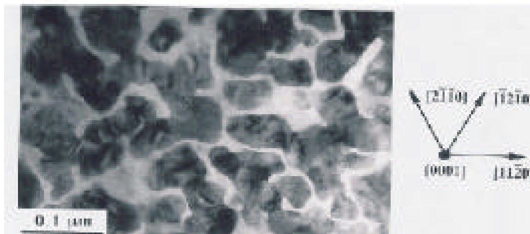

Figure 12. Bright field PTEM micrograph of α-GaN on (111) Si deposited for 30 min. Multi-beam conditions.

Figure 13. Bright field XTEM rnicrograph of a Fig. 12 sample. The GaN and Si are viewed in the [11 $\bar{2}$ 0] and [1 $\bar{1}$ 0] projections, respectively. Multi-beam conditions.

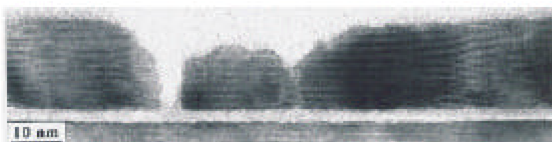

Figure 14. HRXTEM micrograph of a Fig. 12 sample. The GaN and Si are viewed in the [11 $\bar{2}$ 0] and [1 $\bar{1}$ 0] projections, respectively.

these big islands, most of their peripheries are along the <11 $\bar{2}$ 0> directions. This suggests that more deposition of GaN will induce the island-island coalescence by contacting the <11 $\bar{2}$ 0> oriented peripheries, leaving behind sub-boundaries along the <11 $\bar{2}$ 0> orientation. Figure 13 indicates an XTEM micrograph of a Fig. 12 sample observed along the [11 $\bar{2}$ 0] direction of α-GaN. Interesting features of islands at this stage are that each island shows a flat (0001) surface and almost perpendicular edge to the substrate without a specific facet formation. At the positions indicated by arrows in the figure, we can see the formation of sub-boundaries, which would be formed by the island-island coalescence. Figure 14 shows another example of HRXTEM micrographs of the same stage, indicating two islands which just coalesced and formed the sub-boundary. These results well coincide with the formation and arrangement of dislocations forming cell structures as stated in Fig. 4. Thus, the main reason for the formation of high-density threading dislocations is thought to be due to the island-island coalescence at an early stage of growth. During growth at a temperature of 800 °C, small islands will migrate to adjust their orientation each other, resulting in escaping some dislocations out of islands. With the increase of deposition, island size increases accompanying by coarsening sub-boundaries (Figs. 2 and 4). This means the reduction of dislocation densities with the increase of film thickness.

7. Conclusions

The structure and quality of GaN films grown on (111) Si having a 2-3 nm thick amorphous SiN layer by ECR plasma-assisted MBE were investigated under various growth conditions by using transmission electron microscopy. Under optimum growth conditions of representative growth parameters such as ECR plasma power (350 W), N_2 gas flow rate (2 sccm), Ga cell temperature (1041 °C), substrate temperature (800 °C) and nitridation time (5 min), (0001) α-GaN films were epitaxially grown on the above-mentioned substrates with an epitaxial relationship of [11 $\bar{2}$ 0]*GaN* // [1 $\bar{1}$ 0]*Si* and [1 $\bar{1}$ 00]*GaN* // [11 $\bar{2}$]*Si*. The films thus grown included a high density of pure-edge dislocations which were considered to be introduced to relax in-plane misorientations between small angle grain boundaries. It was also confirmed from observations of island-island coalescence stages that the introduction of dislocations is induced along the <11 $\bar{2}$ 0> directions. Under being out of optimum growth conditions, grown layers showed uneven surface and consisted of randomly oriented grains with an average size of 0.1 μm. Moreover, with the decrease of the effective ratio of N_2^* in N_2 gas, the growth of (111) ß-GaN was remarkably observed together with polycrystal α-GaN. An optimum nitridation time to form an optimum amorphous SiN layer on Si was needed to

obtain good results. A "pinhole" model, which explains how heteroepitaxial growth was realized through such a thin amorphous layer formed on the substrate, was proposed. Further study is necessary to clarify this mechanism.

Acknowledgements

MT thanks to the Patrimonial Cathedra program of CONACyT-Mexico. He also acknowledges the help and support of TEM experiments from Nancy Castillo.

References

[1] R. Graupner, QiYe, T. Warwick, and E. Bournet-Courchesne, *J. Cryst. Growth* **217**, 55 (2000), *and references therein.*

[2] Nikishin, N. Faleev, G. Antipov, S. Francoeur, A. Seryogin, M. Holtz, I. P Rokofyeva, S. N. G. Chu, S. Zubrilov, A. Elyukhin, P. Nikitina, A. Nikolaev, Y. Melnik, V. Dmitriev, and H. Ternkin, MRS Internet J. Nitride Semicond. Res. **5S1**, W8.3 (2000), *and references therein*.

[3] Y. Nakada, I. Aksenov, and H. Okumura, Appl. Phys. Lett. **73**, 827 (1998).

[4] W. C. Hughes, W. H. Rawland Jr., M. A. L. Johnson, J. W. Cook Jr., J. F. Schetzina, J. Ren, and J. A. Edmond, J. Vac. Sci. Technol. **B13**, 1571 (1995).

[5] T. Yodo, H. Ando, H. Tsuchiya, D. Nosei, M. Shimeno, Y. Harada, M. Furusawa, and M. Yoshimoto, *Proc. Int. Workshop on Nitride Semicond. IPAP Conf Series* **1**, 351 (2000).

[6] R. J. Molnar and T. D. Moustakas, J. Appl. Phys. **76**, 4587 (1994).

[7] T. Yodo, H. Tsuchiya, H. Ando, and Y. Harada, Jpn. J. Appl. Phys. **39**, 2523 (2000).

[8] D. M. Follstaedt, J. Han, P. Provencio, and J. G. Fleming, MRS Internet J. Nitride Semicond. Res. **4S1**, G3.72 (1999).

[9] H. Lahreche, P. Vennegues, O. Tottenreau, M. Laugt, P. Lorenzini, M. Leroux, B. Beaumont, and P. Gibart, J. Cryst. Growth **217**, 13 (2000).

[10] S. Guha and N. A. Bojarczuk, *Appl. Phys. Lett.* **72**, 415 (1998).

[11] X. H. Wu, L. M. Brown, D. Kapolnek, S. Keller, S. P. DenBaars, and J. S. Speck, J. Appl. Phys. **80**, 3228 (1996).

[12] Y. Shimizu, T. Tominari, S. Hokuto, Y. Chiba, and Y. Nanishi, Jpn. J. Appl. Phys. **37**, L 700 (1998).

[13] Y. Hiroyama and M. Tamura, Jpn. J. Appl. Phys. **37**, L630 (1998).

[14] Akiyama, Y. Kawarada, and K. Kaminishi, Jpn. J. Appl. Phys. **23**, L843 (1984).

[15] Akasaki, H. Amano, Y. Koide, K. Hiramatsu, and N. Sawaki, J. Cryst. Growth **98**, 209 (1989).

[16] M. Ishida, H. Ohyama, S. Sasaki, Y. Yasuda, T. Nishinaga, and T. Nakamura, Jpn. J. Appl. Phys. **20**, L541 (1981).

Appendix

Pinhole model for the epitaxial growth of GaN on amorphous SiN layer

The model is based on the presence of very small micro-pinholes on the SiN layer, as is illustrated in Fig. A1. The size of these pinholes could be in the order of ~10 Å. These pinholes could be the result of a lack of SiN growth on specific sites on the Si surface. These sites could be associated to defects, etc. on the Si surface where N atoms are difficult to bond. The density of these micro-pinholes would depend on the Si surface crystal perfection, on the nitridation conditions, etc.

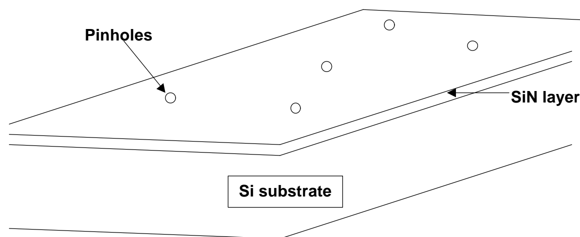

Figure A1

It is worth to comment that holes in the order of ~10 Å in diameter have been observed during the thermal decomposition of a SiO_2 layer on Si. The formation of these holes was attributed to the presence of intrinsic defects like micropores or extrinsic defects like metal impurities on the Si surface.*)

After the nitridation process, with a flux of Nitrogen impinging on the substrate, the GaN growth starts when the Ga cell shutter is opened. Ga atoms would find difficult to bond on the SiN amorphous layer, so they diffuse on the surface until finding a pinhole. Therefore the pinholes become GaN nuclation centers. This is schematically illustrated in Fig.A2.

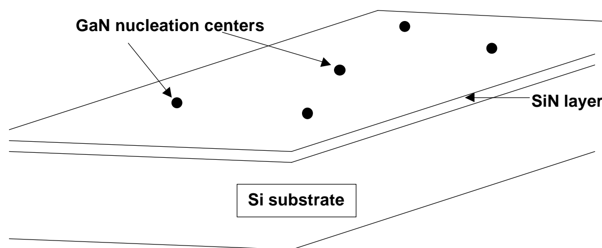

Figure A2

The GaN nuclei fill the micro-pinholes, and start to grow laterally trapping the diffusing Ga atoms on the surface. Again, no GaN grow directly on the SiN surface (Fig. A3).

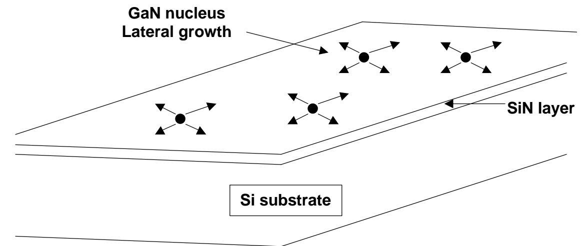

Figure A3

The nuclei become GaN islands growing in the vertical and lateral directions. As a result of the lateral growth GaN epitaxial material is deposited on the amorphous SiN layer, as illustrated in Fig. A4.

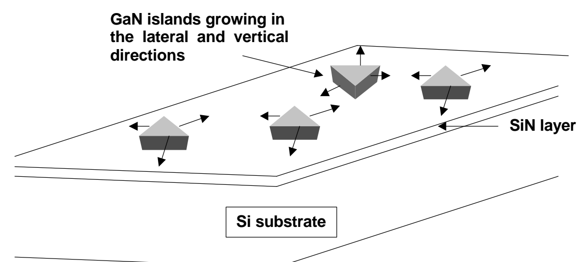

Figure A4

When the islands become larger they start to coalesce as observed in the TEM pictures of Figs. 12-14, and schematically described in Fig. A5. The important point in this model is that in order to obtain GaN epitaxial growth on the SiN amorphous layer, very small micro-pinholes are necessary. The epitaxial information is then transmitted by the lateral growth of GaN, and not by the direct growth on the amorphous SiN layer.

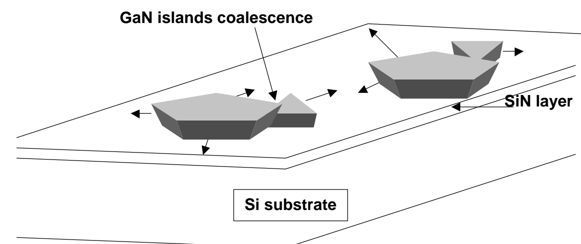

Figure A5

*) R. Tromp, G.W. Rubloff, P. Balk, F.K. LeGoues, and E. J. van Loenen, Phys. Rev. Lett **55**, 2332 (1985).